Investigation of Photocatalytic Activity of TiO2 Nanoparticles Synthesized By Sol-Gel Technique

R. S. Gedam (rupesh_gedam@rediffmail.com)
Visvesvaraya National Institute of Technology
G. K. Sukhadeve
Visvesvaraya National Institute of Technology
S.Y. Janbandhu
Visvesvaraya National Institute of Technology
S. Upadhyay
Visvesvaraya National Institute of Technology

Research Article

Keywords: TiO2 nanoparticles, Absorption study, PL study, indigo carmine dye, Photodegradation

Posted Date: April 27th, 2021

DOI: https://doi.org/10.21203/rs.3.rs-453944/v1

Investigation of photocatalytic activity of TiO_2 nanoparticles synthesized by sol-gel technique

G. K. Sukhadeve, S.Y. Janbandhu, S. Upadhyay, R. S. Gedam*
Department of Physics, Visvesvaraya National Institute of Technology, Nagpur-440010, India
*Corresponding author :- rupesh_gedam@rediffmail.com

Abstract

Anatase phase TiO_2 nanoparticles were synthesized by sol-gel method using titanium(IV) butoxide as a starting material. The pH of solution was maintained by adding HNO_3 and NaOH. The obtained powder was heat treated at 350° C for 2 hours. The XRD study shows that the crystalline size and crystalinity of samples increases with pH of solution. Raman spectra confirm the dominance of anatase phase of TiO_2. Morphology study of samples was done by scanning electron microscope (SEM). The size of prepared samples was calculated by XRD and confirmed by TEM analysis. The energy band gap was calculated by optical absorption spectra and it was found to decrease by increasing pH of the solution. The photodegration activity of IC dye under visible light irradiation was carried out by synthesized TiO_2 Nanoparticles.

Keywords: TiO_2 nanoparticles; Absorption study; PL study; indigo carmine dye; Photodegradation.

1 Introduction

In present days, the wastewater from industries found colorful liquid/dye which contains aromatic rings, metallic and halide ions; which are toxic to human health as well as aquatic life[1]. Such toxic water from industries is directly sent to the nearby rivers, ponds, lakes which reduces the quality of water[2]. There are various methods in order to remove colorants from wastewater such as adsorption, flocculation, ozonation, and photocatalysis. Among all techniques, photocatalysis is a low-cost, ecofriendly, efficient, and reusable to decompose colorants[3,4]. There are several metal oxide nanoparticles used as a photocatalyst because of their different physical and chemical properties better than bulk materials[5]. In semiconductor

nanomaterial, due to small size motion of charge carriers is controlled by quantum confinement[6].Large surface area of nanoparticles is useful in making interaction between material and medium. SpeciallyTiO_2 had been studied widely as a photocatalyst due to its great photochemical activity, non-toxicity, low-cost production, and high dielectric constant. Also, the oxygen atoms on surface of TiO_2 takes part in oxidation-reduction reaction[7,8].

TiO_2 is synthesized by several methods like sol-gel,hydrothermal, CVD, microwave, ball milling, etc[9–12].Among all these methods sol-gel process is the most interesting and easy method. It requires low temperature, easy process, high degree of purity and homogeneity. It is also advantageous to regulate grain size, crystalline size, and morphology. However,TiO_2 has three crystalline phases namely anatase, brookite, and rutile. Among these three phases, rutile is stable while brookite and anatase are metastable phases[13]. The high photoreactivity of $TiO_2$is obtained in anatase phase which is metastable. The present work is to synthesis anatase$TiO_2$and study the effectof pH on crystalline size, morphology, and optical properties. Also to use prepare TiO_2 for degradation of IC dye.

2 Experimental

TiO_2nanopowder was prepared by simple sol-gel method. Titanium (IV) butoxide (supplied by Sigma-Aldrich 97%) was used as Ti precursor, Titanium (IV) butoxide (40 mmol) was mixed with ethanol (50ml). After mixing, it was stirred magnetically for 45 min at room temperature. In another beaker, a solution of deionized water (having different pH = 1,3,5) and ethanolwas taken to use as a catalyst to promote hydrolysis. The pH of solution was maintained by adding HNO_3(supplied by Sigma-Aldrich 65%) or NaOH. Mixture of deionized water and ethanol was added drop-wise in a precursor solution, during this process precursor solution was heated upto 50℃ and the temperature was maintained during the reaction. This solution was stirred for 3 hours which gives clear white solution. The obtained sol was kept for gel formation for 24 hours at room temperature which gives high viscous suspension. This viscous suspension was then washed with ethanol and deionized water for several times and dried at 90℃ for 15 hours in a vaccum which gives a white powder. The various powder samples of TiO_2 were prepared by maintaining the different pH of the solution (pH= 1, 3, 5). The prepared samples wereheat-treated at 350°C for 2hours and named as p1_350, p3_350, and p5_350.

3 Characterization of TiO_2

Crystalline nature of powder sample was studied by XRD (Bruker AXS D8 Quest System) using Cu as a target (CuKα1=1.5406Å) at 40mA and 45Kv.XRD measurement was carried out in the range from 15 to 80 degrees with a step size of 0.017. The Raman spectra of samples was recorded using Raman Spectrometer (NOST: HEDA-URSM4/5/7). Morphological study of sample was done using scanning electron microscope (SEM – ZEISS EVO18). The TEM analysis was carried out using TEM – Thermofisher:Talos F200 S. Absorption spectra of TiO_2powder sample and photocatalytic activity of Indigo Carmine dye were recorded using UV-Vis NIR spectrophotometer (JASCO, V-670). Photoluminescence spectra (PL) was recorded using JASCO FP-8200 spectrofluorometer.

4 Photocatalytic Degradation of IC Dye

The catalytic performance of prepared TiO_2 nanoparticles was studied for degradation of IC dye (10ppm) as a pollutant under the irradiation of visible light. Degradation was performed in self made reactor under irradiation of 12 lamps of 100W each. The temperature of reactor was maintained using air circulating fans. For photocatalytic experiment, 100ml aqueous solution of IC dye was taken in beaker, and 0.06 gm of catalyst was added in solution. After adding a catalyst, initially the solution was stirred in dark for 30min to attain adsorption- desorption equilibrium between the catalyst and dye solution. After this whole setup was brought into self made reactor, where photocatalysis reaction was started by irradiation of visible light. During the reaction, 3 to 4ml of solution was taken out after an interval of 7 minute and centrifuged. The solution was thenanalysed using UV-vis-NIR spectrophotometer (JASCO V-670) at room temperature.

5 Results and Discussion

5.1 XRD Analysis:

Diffraction pattern of prepared TiO_2 is shown Fig.1.This XRD pattern shows high intensity peak (110) at 25.3°, which confirms the formation of crystalline anatase phase of TiO_2 (PDF NO. 01-275-2545) with tetragonal crystal structure and having primitive lattice with lattice

parameter a = 3.79900Å and c = 9.50900Å. It is also observed that intensity of the XRD peaks increases with pH and it is maximum for pH 5.

The other XRD peaks at 37.90, 48.04, 54.17, 55.18, 62.78, 69.56, and 75.45 corresponds to (004), (200), (105), (211), (204), (215), (116) planes of anatase phase of TiO_2[14,15]. It is confirmed that the crystallites size of TiO_2 is found to grow with increase in pH value.

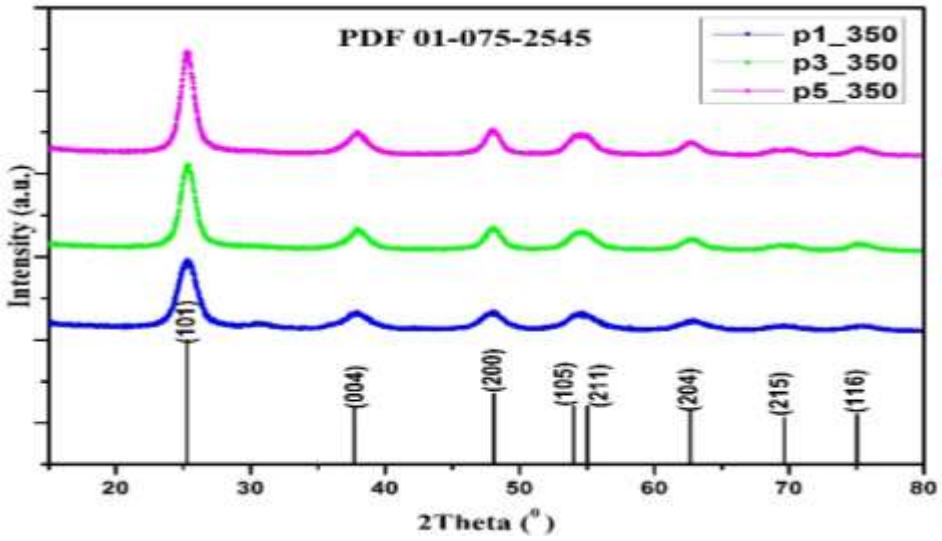

Fig. 1 XRD pattern of TiO_2

The crystalline size of prepared powder have been calculated by DebeyScherrer formula and depicted in table 1.

$$D = \frac{k\lambda}{\beta \cos\theta} \ldots\ldots(1)$$

where $\beta = (FWHM) \times (\pi / 180)$,is the broadening ($\beta$= 0.02390 is the value of prepared sample) at half of the maximum intensity (FWHM), after subtracting instrumental line broadening in radian,λ is the X-ray wavelength of the incident radiation (The crystallinity of prepared NTO was analyzed by X-ray diffractometer using $Cu\text{-}K\alpha$ radiation of wavelength 1.5060 Å),θ is the Bragg's diffraction angle and K = 0.9 is a dimensionless shape factor, called Scherrer's constant.

Table 1 crystalline size of TiO_2

Sr no.	Sample Id	Crystalline size (nm)
1	p1_350	4.8 nm
2	P3_350	6.5 nm
3	p5_350	7.0 nm

From table 1 it is observed that the size of TiO_2 crystallites increases with increase in pH of solution[16].

5.2 Raman Spectra:

Fig.2 Illustrates the Raman spectra of the samples heat treated at 350° C for 2 hours. The observed Raman peaks corresponds to the anatase phase of TiO_2. In anatase phase of TiO_2, six active Raman modes (3Eg + 2B1g+A1g) are observed[17]. For all samples the peaks at 144 cm^{-1} (Eg), 197 cm^{-1} (Eg), 399 cm^{-1} (B1g), 517 cm^{-1} (A1g+B1g) and 639 cm^{-1} (Eg) are very well matched with the reported data[18]. It is observed that intensity of Raman peaks decreases with pH of the solution. The band at 517 cm^{-1} is due to the stretching of Ti-O type vibrations hence it shows two Raman modes[19]. Although the samples were prepared by maintaining different pH, no change in the peak position is observed which confirms the absence of impurity in all the prepared samples.

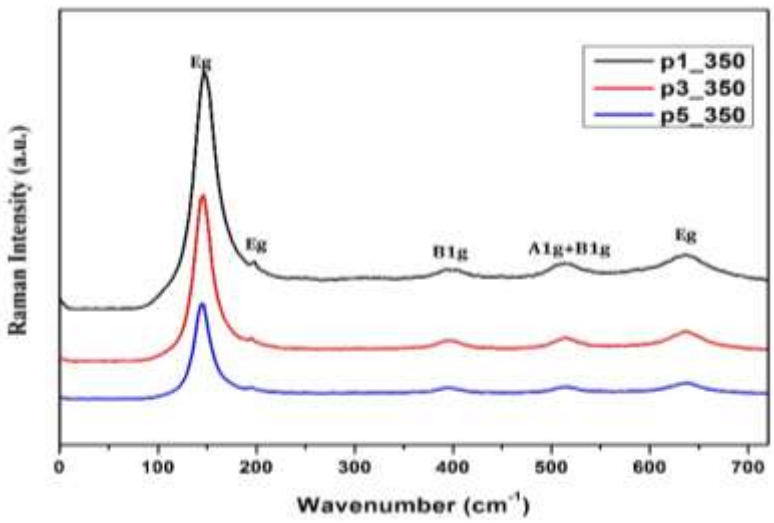

Fig. 2 Raman Spectra of prepared Samples

5.3 Morphology of TiO_2 :

Fig. 3 (a, b, and c) depicts the SEM images of TiO_2 nanoparticles prepared at different pH (1, 3, and 5) and heat treated at 350ºC for two hours. SEM image of sample p1_350 (fig. 3.a) shows that the particles are very small and because of the smaller size, particles are seen to be agglomerated.SEM images(fig. 3.b,c) of p3_350 and p5_350 are less agglomerated as compared to p1_350 may be due to larger size crystallites[20]. The observed results shows that size of TiO_2 crystallites increases with pH which is supported by XRD data.

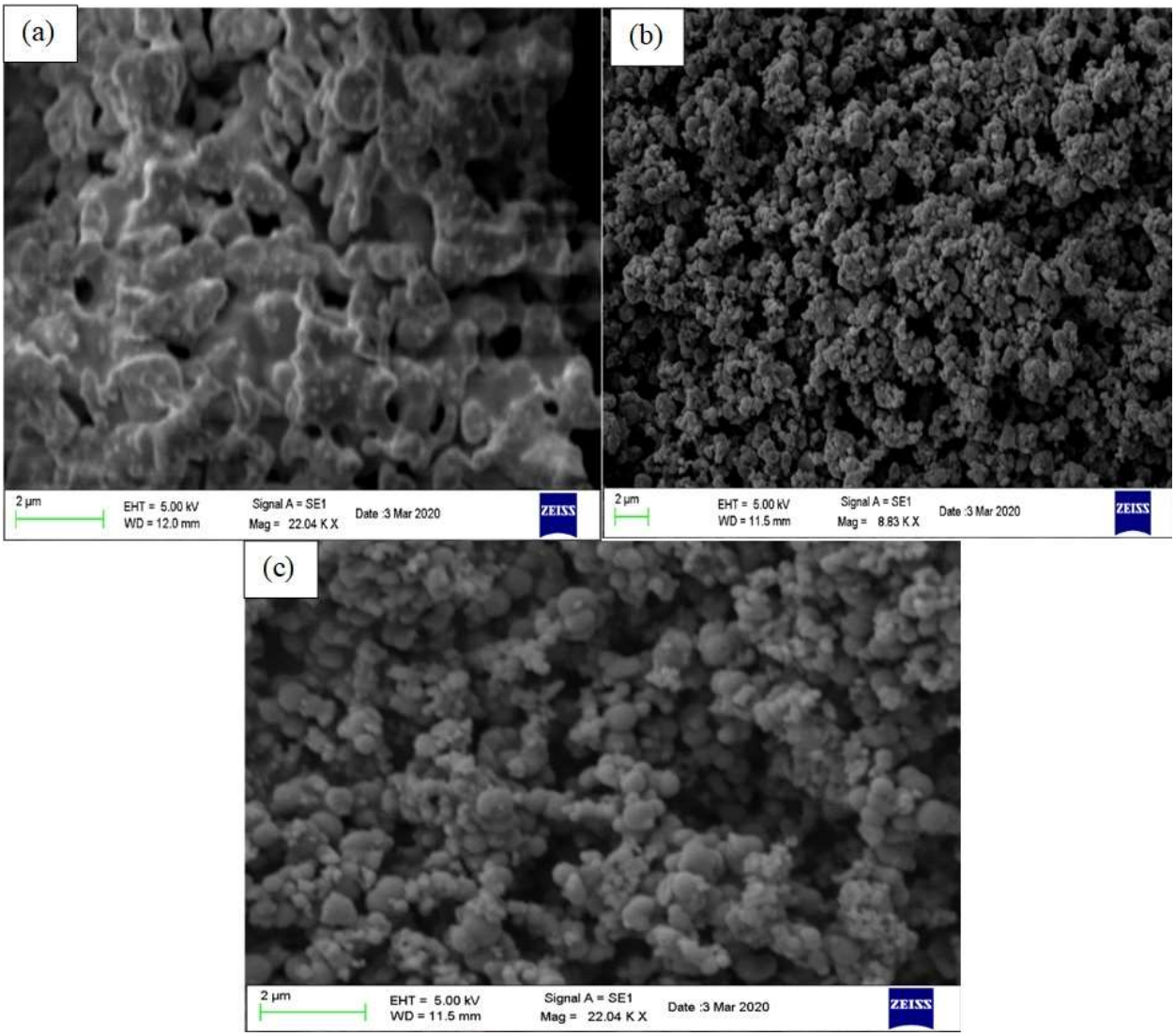

Fig.3 SEM images of TiO2 nanoparticles **(a)** p1_350, **(b)** p3_350 and**(c)** p5_350

5.4 TEM Analysis:

Fig 4(a) shows the TEM image of sample p1_350. It is observed from TEM image that the prepared TiO_2 nanoparticles have non-homogeneous distribution and the average size of the TiO_2 nanoparticles is found to be 7nm[8]. Fig 4(b) shows the SAED pattern of p1_350, which confirms the prepared powder is crystalline in nature and it comprises the anatase phase of TiO_2. In SAED pattern rings are assigned to (110), (004) and (200) plane of anatase TiO_2 which are in good agreement with the XRD results. The lattice spacing between the lattice plane was found to be 0.34nm which corresponds to (110) plane of anatase TiO_2 (fig 4.c). The presence of Ti and O in the synthesized material is confirmed by EDS spectra (fig 4.d).

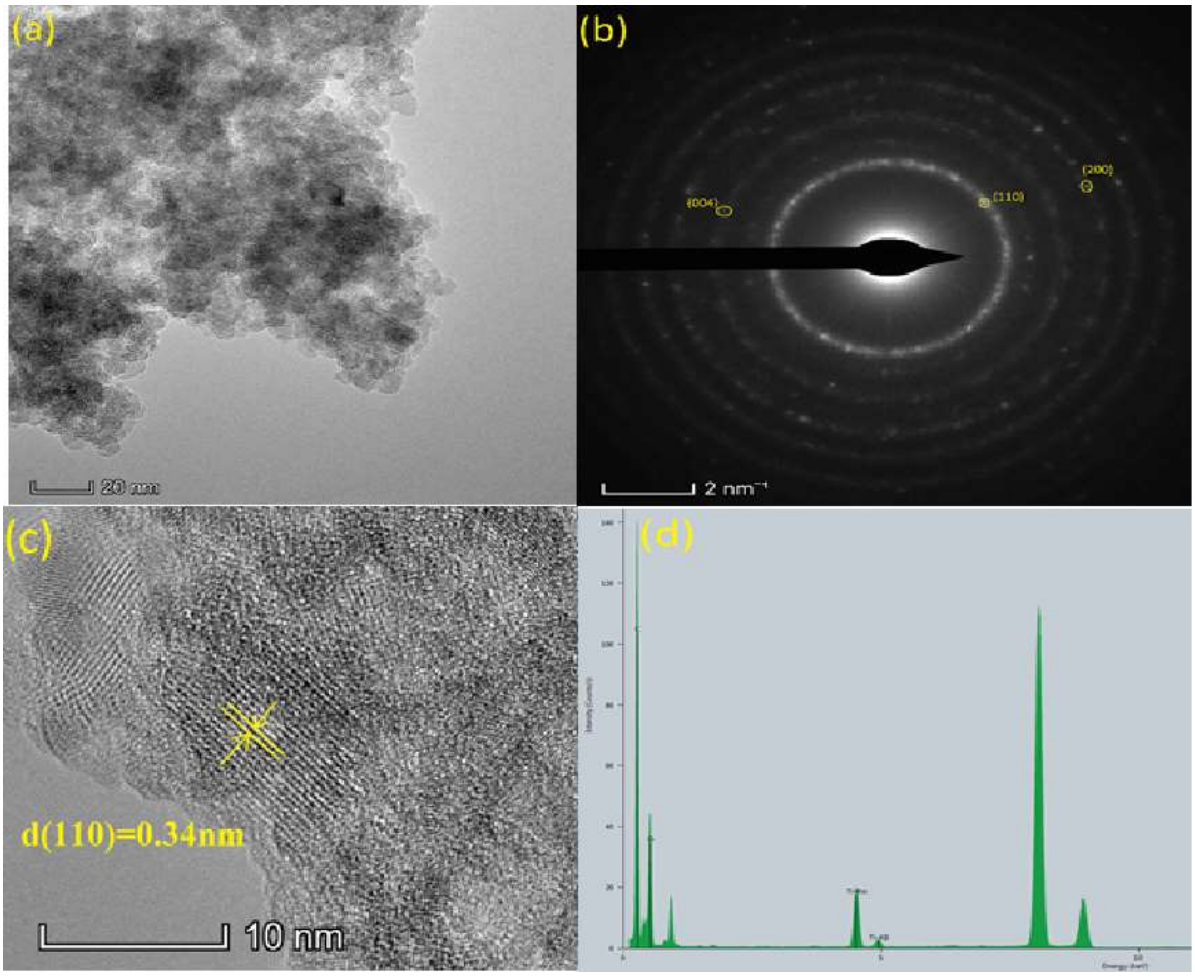

Fig.4 (a) TEM image**(b)** SAED pattern **(c)** IFFT **(d)** TEM-EDAX of p1_350.

5.5Absorption Spectra

Absorption spectra of synthesized TiO_2 powder is shown in fig.5. From this spectrum it is observed thatcut off wavelengthshifts to the higher wavelength with increase in pH. The shift in absorption edge towards longer wavelength may be due to increase in particle size of TiO_2[21].

The optical energy band gap of prepared samples was calculated by Tauc plot using equation

$$(\alpha hv)^n = A(hv - E_g) \quad \ldots\ldots\ldots\ldots\ldots\ldots (2)$$

where, α is absorption coefficient, hv is photon energy, A is the constant depend on material, n is the value which is related to the transition (n=2 for direct bandgap, 2/3 for direct forbidden bandgap, and ½ for indirect bandgap).

The plot of $(\alpha hv)^2$ v/s hv i.e. Tauc plot (fig.6)gives direct bandgap energy. The obtained direct bandgap energies of samples was calculated by extrapolating to hv axis i.e. to $\alpha = 0$ and depicted in table2[22]. From this table, it is observed that the energy bandgap decreases with increase inpH. This decrease in energy bandgapof TiO_2 may be due to increase in crystalline size of TiO_2nanoparticle which is also supported by XRD results. The bandgap of semiconductor is size dependent, hence decrease in bandgap by increasing pH of solution related to increase in crystalline size[8,20].

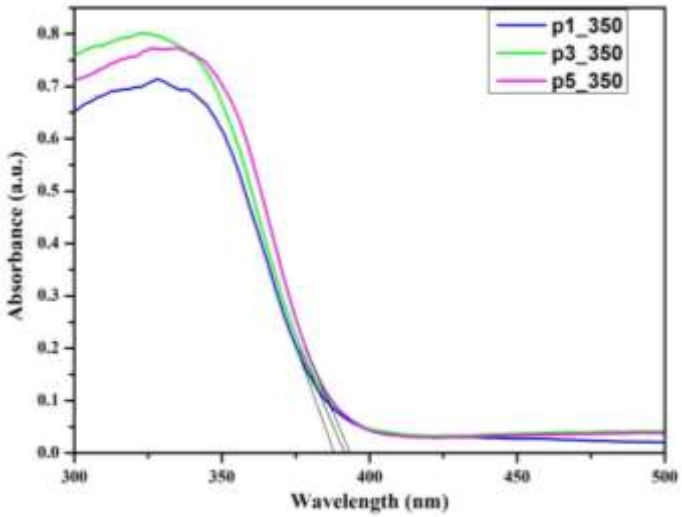

Fig. 5 Absorption Spectra of TiO_2

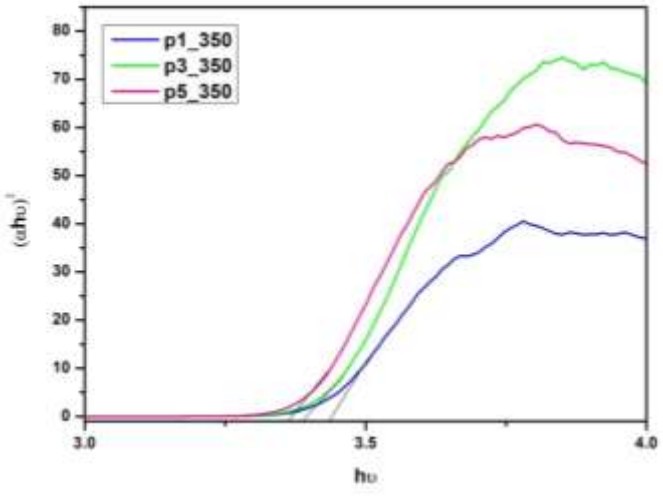

Fig. 6 Tauc of TiO_2

Table 2 Energy band gap TiO_2 nanoparticles

Sr no.	Sample Id	Band gap (eV)
1	p1_350	3..43 eV
2	P3_350	3.38 eV
3	p5_350	3.30 eV

5.6 PL spectra of TiO_2

The PL spectra is used to investigate electronic structure, recombination and transfer of electron hole pair in semiconductor[23]. Fig.7depicts the PL spectra of TiO_2 excited at 300nm. The PL spectra was recorded at room temperature in wavelength range 320 to 550nm.It is observed from the spectra that sample with pH=1 (p1_350) shows very less intensity peak due to less recombination of electron-hole pairs. As the pH value of the solution increases to 3 the PL intensity is found to increase. This increase in intensity is due to more recombination of electrons and holes. For samples p5_350 the intensity is intermediate to that of the p1_350 and p3_350samples. Observed peaks in PL spectra of TiO_2 are may be due to self trappedexcitons, oxygen vacancy and surface defects[18,24–26]. The band edge emission of 382 nm may be due to recombination of excitons[27]. The peak observed at 397nm for all samples is due to the indirect transition$\Gamma_{1b} \rightarrow X_{2b}$, and the blue emission peak was found at 450nm[28–30]. The peak at 468nm is due to the electron trapped from defect level and oxygen vacancy[31]. The peaks on higher wavelength side i.e. at 482nm and 494nm are due to oxygen vacancy and transition from $Ti^{+3}\ to\ TiO_6^{-2}$[29]. The lower PL intensity for sample p1_350 due to decrease in recombination of charge carriers results in improvement of charge separation[32].

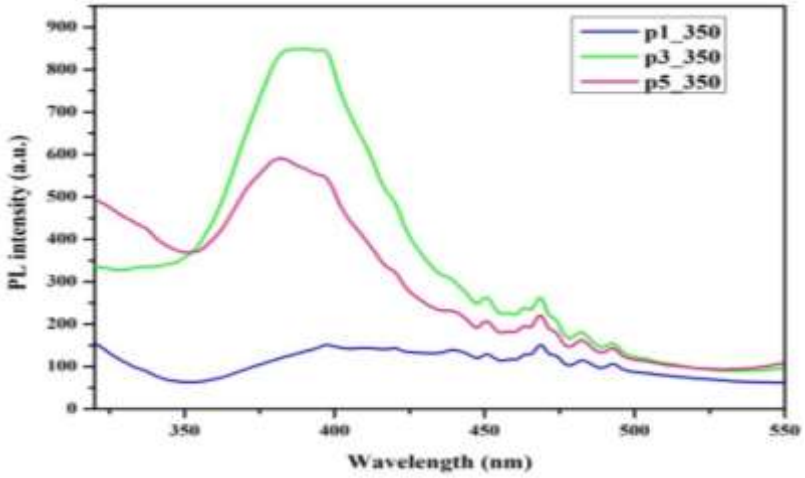

Fig. 7 PL Spectra of TiO_2

6 Degradation measurement of IC dye

It is revived that the materials having less recombination rate of electron and hole shows high photocatalytic activity[32]. Since p1_350 shows low PL intensity among all samples, this sample was chosen to degrade the IC dye under visible light irradiation.

The photocatalytic degradation of the indigo carmine dye of concentration 10 ppm was checked by adding 0.06gm powder of p1_350. Fig.8 depicts the absorption spectra of photodegraded IC suspension over anatasetitania nanoparticles. It was found that, when the solution was stirred in dark there was a small decrease in the intensity of peak. As it was exposed in visible light, the intensity was decreased very rapidly, and after the 21 min of activity the absorption peak become completely flat.IC concentrations throughout the experiment were carried out by observing the intensity of the absorption peak at 611 nm. Decrease in intensity peak at 611 nm was used to determine the degradation efficiency.

The degradation efficiency was calculated using equation

$$\% \text{ degradation} = \left(1 - \frac{C_t}{C_0}\right) X100 \qquad \ldots\ldots\ldots\ldots (3)$$

where, C_0 and C_t are the concentrations of indigo carmine dye solution at time t = 0 and at time t respectively.

Moreover Beer-Lambert law was employed to calculate the concentration of degraded IC solution is given by:

$$C = A/\varepsilon l \ldots\ldots\ldots\ldots\ldots\ldots\ldots\ldots\ldots\ldots (4)$$

where,A is the absorbance detected by graph, ε is the molar absorption coefficient, and l is the optical path length.

The photodegradation efficiency for P1_350@2 was calculated and found to be 87.9 % for 10 ppm IC solution over a period of 21 minutes under UV-visible light irradiation.

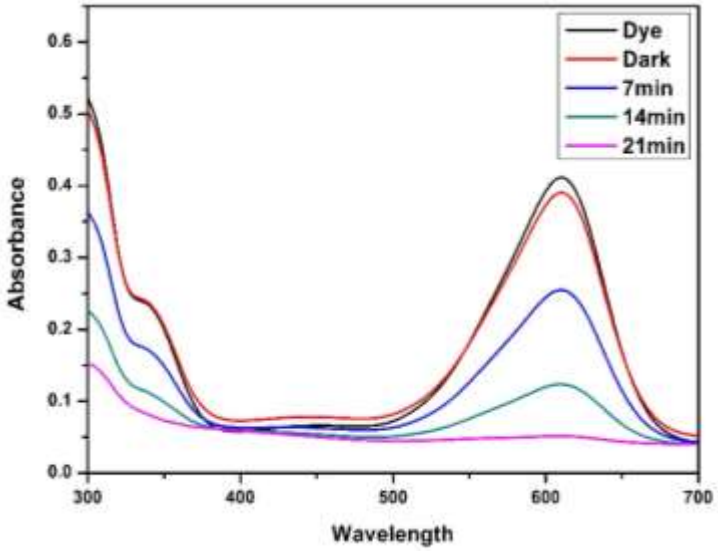

Fig. 8 Absorbance spectra of IC dye

6.1Optimization of catalyst dose

The degradation efficiency was studied by increasing the catalyst dose. Fig.9 shows the effect of catalyst dose on the degradation efficiency of IC dye. From this figure it is observed that for catalyst dose of 0.02gm the degradation efficiency was foundto be 81.60% and efficiency found to increase up to 0.06gm. With further increase in catalyst dose beyond 0.06gm degradation efficiency was found to decrease. The variation in degradation efficiency with catalyst dose can be understood on the basis of free radicals. With increase in catalyst dose from 0.02gm to 0.06gm active sites on the surface of catalyst increases which amplifies the free radicals results in more oxidation of IC dye. With further increase in catalyst dose beyond 0.06gm light shielding effect increases which reduces degradation of IC dye[33]. Thus overdose of catalyst decrease the rate of degradation which results in decrease in degradation efficiency.

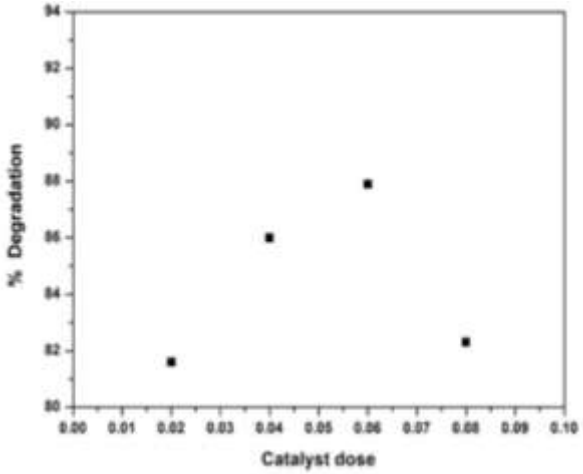

Fig. 9 Effect of catalyst dose on degradation efficiency

The photocatalytic mechanism is initiated by absorbing a photon having energy greater than or equal to 3.2eV (TiO_2band gap) (equ. 5) . The incident photon excite the electron from valance band to conduction band and leaving behind hole in valance band (as shown in fig.10).

$$TiO_2 + h\nu \longrightarrow h^+(TiO_2) + e^-(TiO_2) \quad \ldots\ldots\ldots (5)$$

The hole in valance band undergoes oxidation to oxidized H_2O and gives hydroxyl radical ($OH^\bullet$). This hydroxyl radical will attack the pollutant adsorbed on the surface of catalyst and degrade the pollutant into H_2O and CO_2(equ. 6).

$$h^+ + H_2O \longrightarrow OH^\cdot + H^+ \quad \ldots\ldots\ldots\ldots\ldots\ldots\ldots (6)$$

The electron in conduction band undergoes reduction reaction with dissolving oxygen in water to form superoxide (equ. 7).

$$O_2 + e^- \longrightarrow O_2^{\cdot -} \ldots\ldots\ldots\ldots\ldots\ldots\ldots\ldots (7)$$

The superoxide undergoes multiple reaction to give hydroxyl radical ($OH^\bullet$) (equ 8,9).

$$O_2^{\cdot -} + H^+ \longrightarrow HO_2^\cdot \ldots\ldots\ldots\ldots\ldots \quad (8)$$

$$2HO_2^\cdot \longrightarrow H_2O_2 + O_2 \ldots\ldots\ldots\ldots \quad (9)$$

Finally photogenerated electron attack H_2O_2 to form hydroxyl radical (Equ.10).

$$H_2O_2 + e^- \longrightarrow OH^\cdot + OH^- \ldots\ldots (10)$$

The hydroxyl radical react with IC dye to degrade it and give H_2O and CO_2as a final product (equ. 11).

$$OH^\cdot + IC\ dye \longrightarrow CO_2 + H_2O \ldots\ldots\ldots\ldots \quad (11)$$

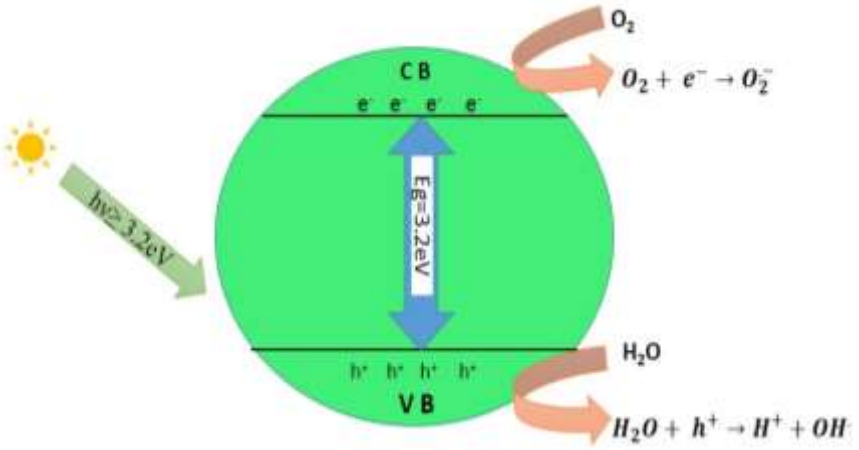

Fig. 10 Mechanism of photocatalysis in TiO_2

7 Conclusion –

TiO_2 nanoparticles were synthesized by sol-gel technique and crystallites were grown by optimized heat treatment schedule. Anatase phase of TiO_2 was confirmed by XRD measurment. The anatase phase of TiO_2 was also supported by Raman spectra. The surface morphology and effect of pH on TiO_2 nanoparticles were studied by SEM. The average size of TiO_2 nanoparticle was calculated from TEM and it was found to be 7nm. The shift in absorption edge due to increase in particle size of TiO_2 was observed in absorption spectra. PL study was carried out to know the recombination of charge carriers at the excitation. Since the recombination of electron and hole was less in p1_350, it was chosen for dye degradation study. The degradation efficiency was found to be 87.9 %. The effect of dose on degradation efficiency was also carried out and it was found to be maximum for 0.06gm. This study shows the prepared TiO_2 can be used for degradation of IC dye.

Acknowledgement

G. K. Sukhadeve is thankful to VNIT, Nagpur (India) for financial help. Authors are thankful to Department of Physics, VNIT, Nagpur for providing Raman facility procured under DST-FIST, New Delhi (GOI). Authors express their sincere thanks to Department of Chemistry, VNIT, Napgurand Department of Physics RTMN University Nagpur for providing XRD and SEM characterization respectively. The authors acknowledge the TEM facility, funded by a TPF Nanomission, GOI project at Centre for Nano and Soft Matter Sciences, Bengaluru.

References

1. A. Castro-Beltrán, P. A. Luque, H. E. Garrafa-Gálvez, R. A. Vargas-Ortiz, A. Hurtado-Macías, A. Olivas, J. L. Almaral-Sánchez, and C. G. Alvarado-Beltrán, Optik (Stuttg). **157**, 890 (2018).

2. S. R. Munishwar, P. P. Pawar, S. Y. Janbandhu, and R. S. Gedam, Opt. Mater. (Amst). **99**, 109590 (2020).

3. P. V. Nidheesh, R. Gandhimathi, and S. T. Ramesh, Environ. Sci. Pollut. Res. **20**, 2099 (2013).

4. U. I. Gaya and A. H. Abdullah, J. Photochem. Photobiol. C Photochem. Rev. **9**, 1 (2008).

5. M. Sorbiun, E. Shayegan Mehr, A. Ramazani, and S. Taghavi Fardood, Int. J. Environ. Res. **12**, 29 (2018).

6. S. R. Munishwar, P. P. Pawar, S. Y. Janbandhu, and R. S. Gedam, Opt. Mater. (Amst). **86**, 424 (2018).

7. W. Buraso, V. Lachom, P. Siriya, and P. Laokul, Mater. Res. Express **5**, 0 (2018).

8. R. S. Dubey, Mater. Lett. **215**, 312 (2018).

9. S. Valencia, J. M. Marín, and G. Restrepo, Open Mater. Sci. J. **4**, 9 (2010).

10. J. Hou, X. Yang, X. Lv, M. Huang, Q. Wang, and J. Wang, J. Alloys Compd. **511**, 202 (2012).

11. S. Gayathri, M. Kottaisamy, and V. Ramakrishnan, AIP Adv. **5**, (2015).

12. J. L. Guimarães, M. Abbate, S. B. Betim, and M. C. M. Alves, J. Alloys Compd. **352**, 16 (2003).

13. F. Z. Haque, R. Nandanwar, and P. Singh, Optik (Stuttg). **128**, 191 (2017).

14. S. K. M. Jose, Appl. Phys. A 1 (2017).

15. S. Y. Janbandhu, A. Joshi, S. R. Munishwar, and R. S. Gedam, Appl. Surf. Sci. **497**, (2019).

16. S. Mahshid, M. Askari, and M. S. Ghamsari, J. Mater. Process. Technol. **189**, 296 (2007).

17. H. C. Choi, Y. M. Jung, and S. Bin Kim, **37**, 33 (2005).

18. H. Tang, H. Berger, P. E. Schmid, F. Lévy, and G. Burri, Solid State Commun. **87**, 847 (1993).

19. T. Ohsaka, F. Izumi, and Y. Fujiki, **7**, 321 (1978).

20. M. Tsega and F. B. Dejene, Heliyon **3**, e00246 (2017).

21. S. R. Munishwar, P. P. Pawar, and R. S. Gedam, J. Lumin. **181**, 367 (2017).

22. S. Y. Janbandhu, S. R. Munishwar, and R. S. Gedam, Appl. Surf. Sci. **449**, 221 (2018).

23. J. Zhang, Y. Yang, and W. Liu, Int. J. Photoenergy **2012**, (2012).

24. L. V. Saraf, S. I. Patil, S. B. Ogale, S. R. Sainkar, and S. T. Kshirsager, Int. J. Mod. Phys. B **12**, 2635 (1998).

25. N. Serpone, D. Lawless, and R. Khairutdinov, J. Phys. Chem. **99**, 16646 (1995).

26. L. Forss and M. Schubnell, Appl. Phys. B Photophysics Laser Chem. **56**, 363 (1993).

27. S. R. Munishwar, P. P. Pawar, S. Ughade, and R. S. Gedam, J. Alloys Compd. **725**, 115 (2017).

28. A. Maurya, P. Chauhan, S. K. Mishra, and R. K. Srivastava, J. Alloys Compd. **509**, 8433 (2011).

29. D. Komaraiah, E. Radha, N. Kalarikkal, J. Sivakumar, M. V. Ramana Reddy, and R. Sayanna, Ceram. Int. **45**, 25060 (2019).

30. M. C. Mathpal, A. K. Tripathi, M. K. Singh, S. P. Gairola, S. N. Pandey, and A. Agarwal, Chem. Phys. Lett. **555**, 182 (2013).

31. A. Saha, A. Moya, A. Kahnt, D. Iglesias, S. Marchesan, R. Wannemacher, M. Prato, J. J. Vilatela, and D. M. Guldi, Nanoscale **9**, 7911 (2017).

32. S. Y. Janbandhu, S. R. Munishwar, G. K. Sukhadeve, and R. S. Gedam, Mater. Charact. **152**, 230 (2019).

33. S. Rani, M. Aggarwal, M. Kumar, S. Sharma, and D. Kumar, Water Sci. **30**, 51 (2016).

Declarations

Funding : No funding is available.

Declaration of Competing Interest:

The authors declare that they have no known competing financial interests or personal relationships that could have appeared to influence the work reported in this paper.

Figures

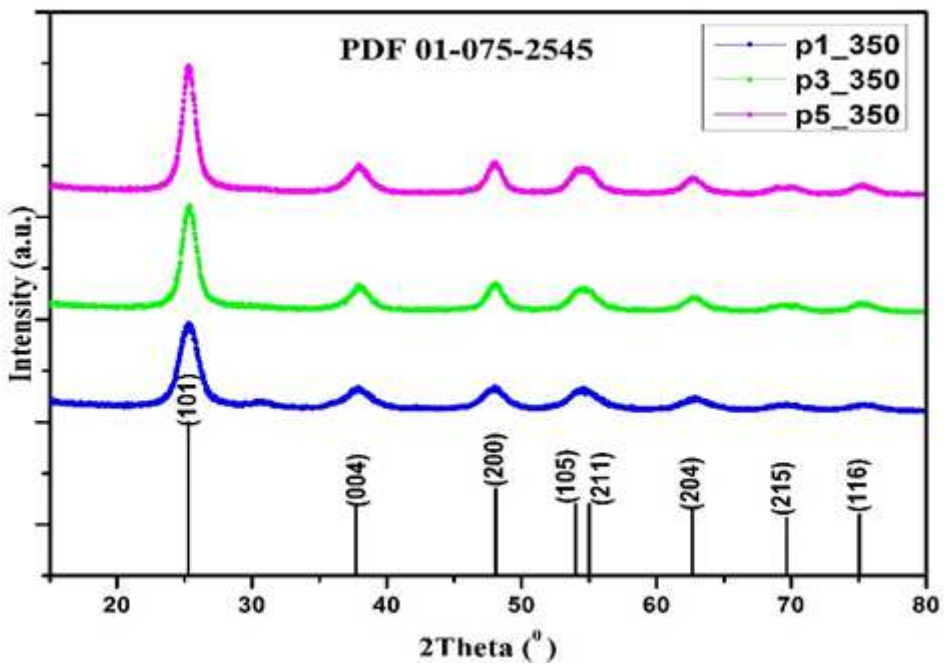

Figure 1

XRD pattern of TiO2

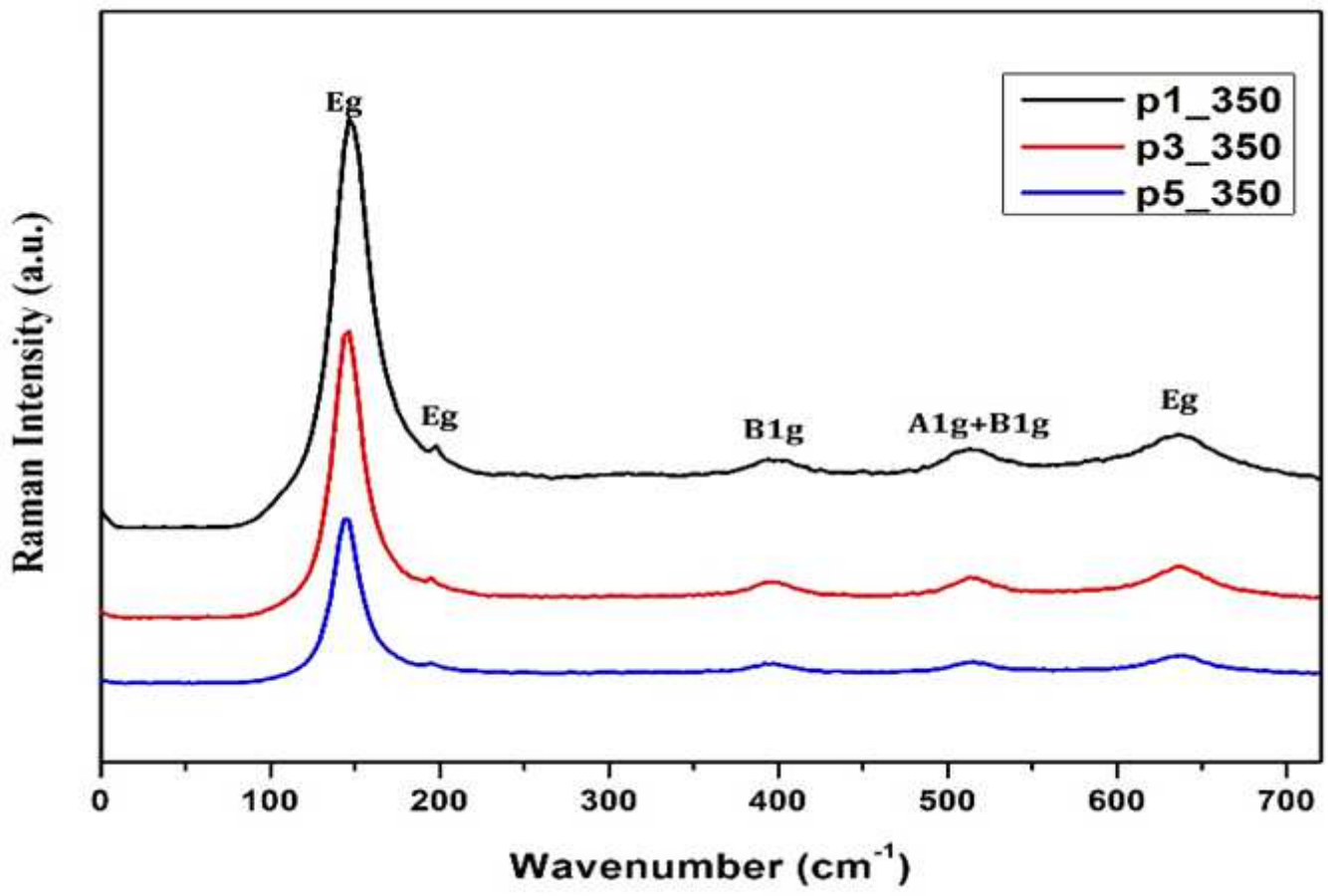

Figure 2

Raman Spectra of prepared Samples

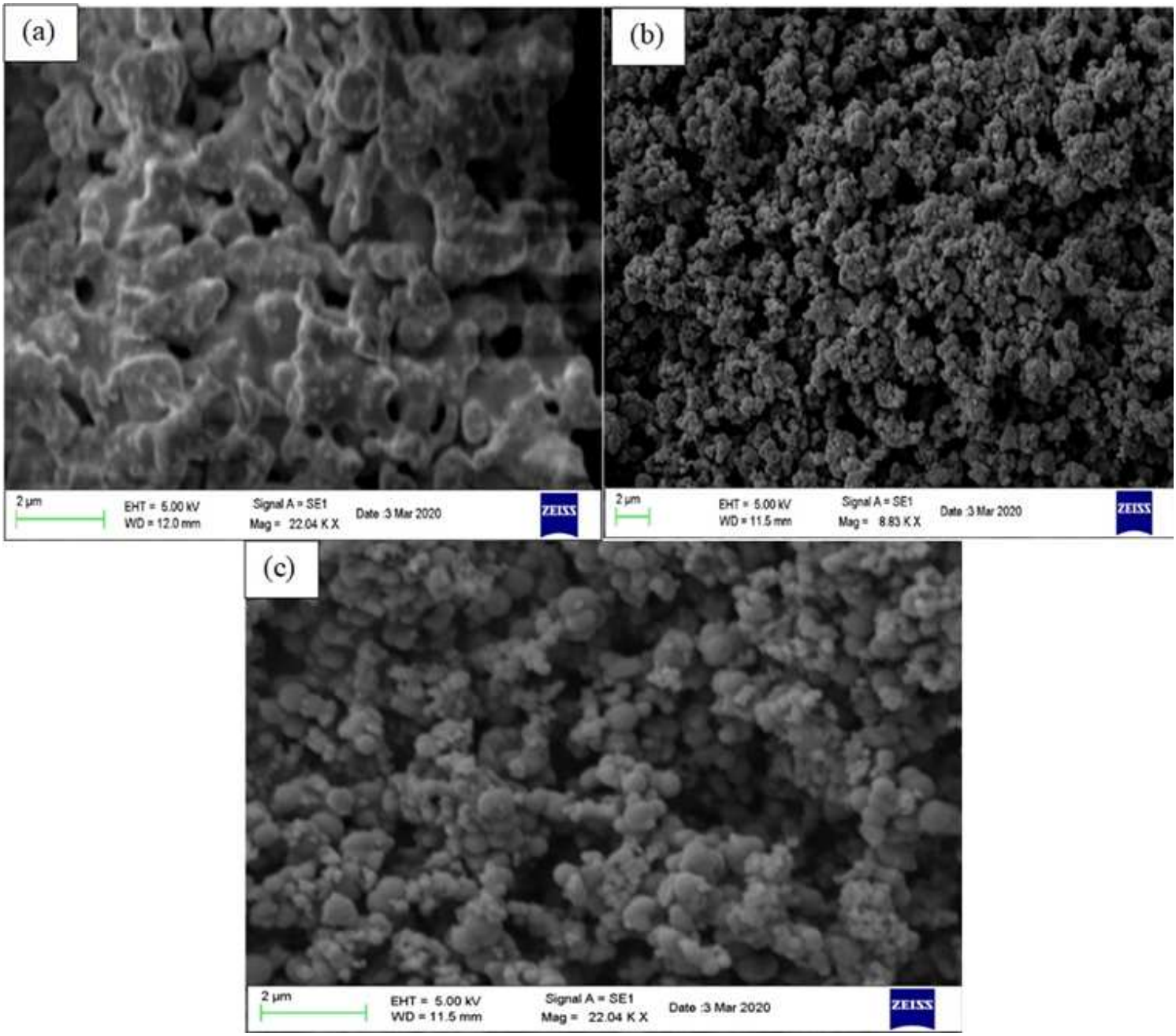

Figure 3

SEM images of TiO2 nanoparticles (a) p1_350, (b) p3_350 and(c) p5_350

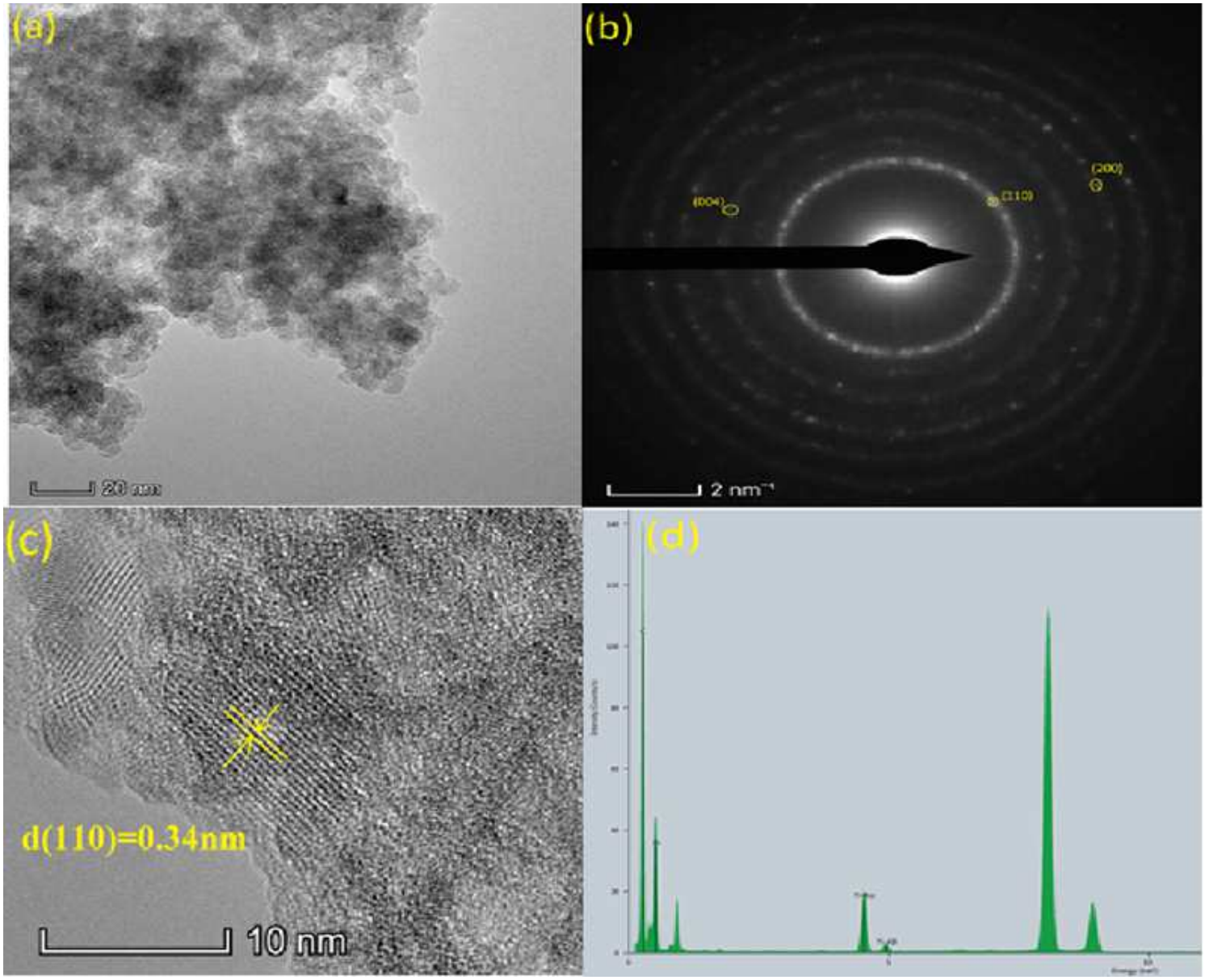

Figure 4

(a) TEM image(b) SAED pattern (c) IFFT (d) TEM-EDAX of p1_350.

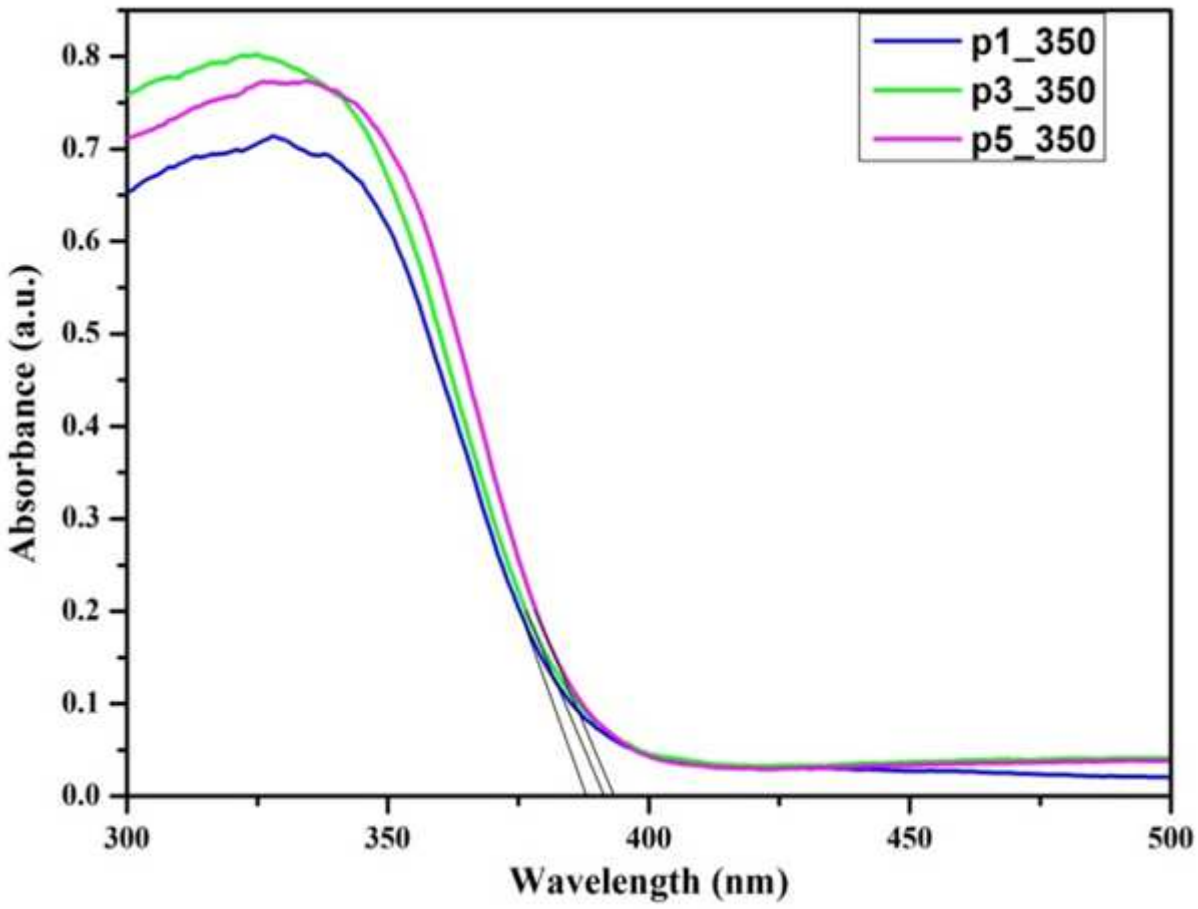

Figure 5

Absorption Spectra of TiO2

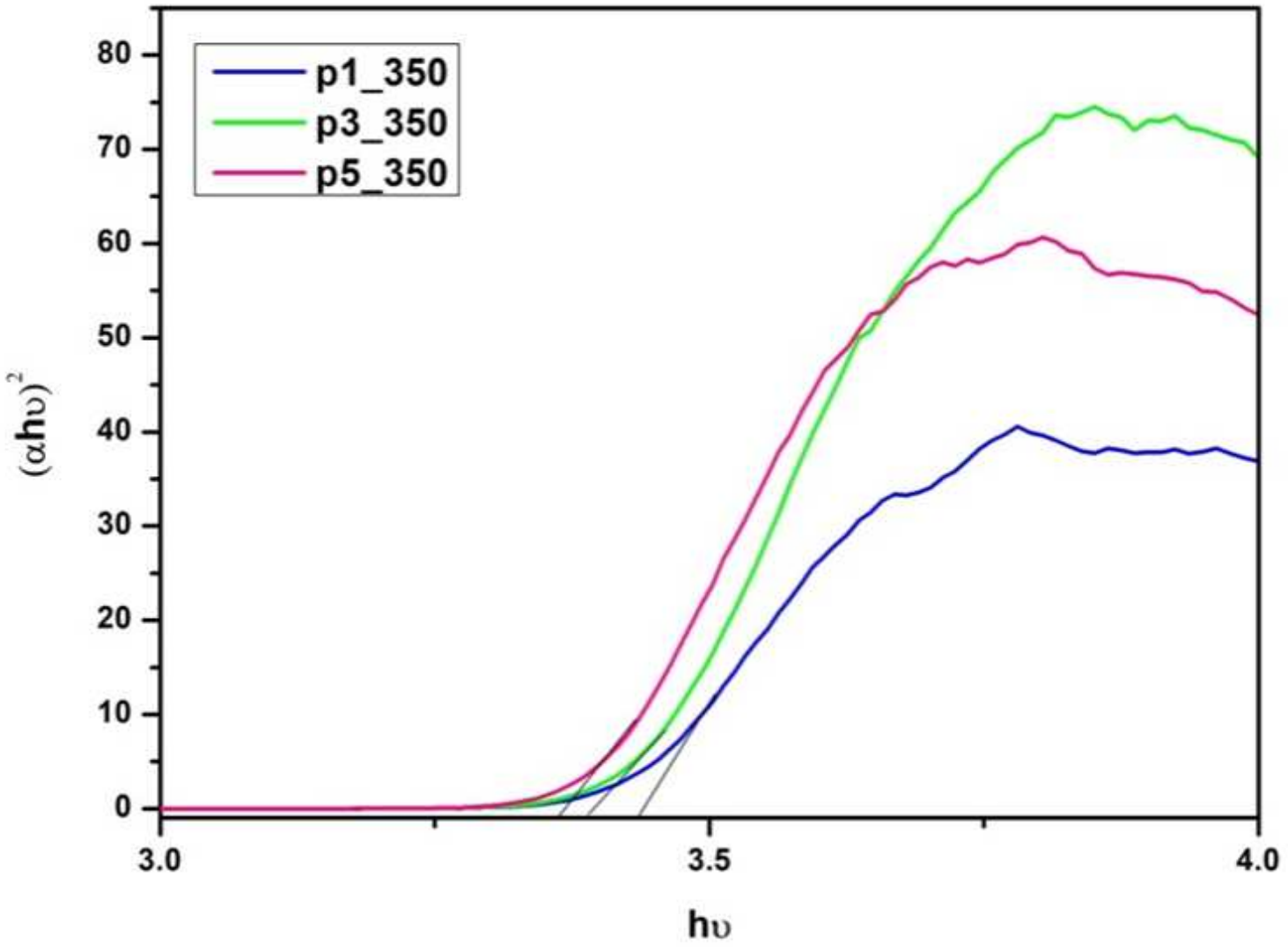

Figure 6

Tauc of TiO2

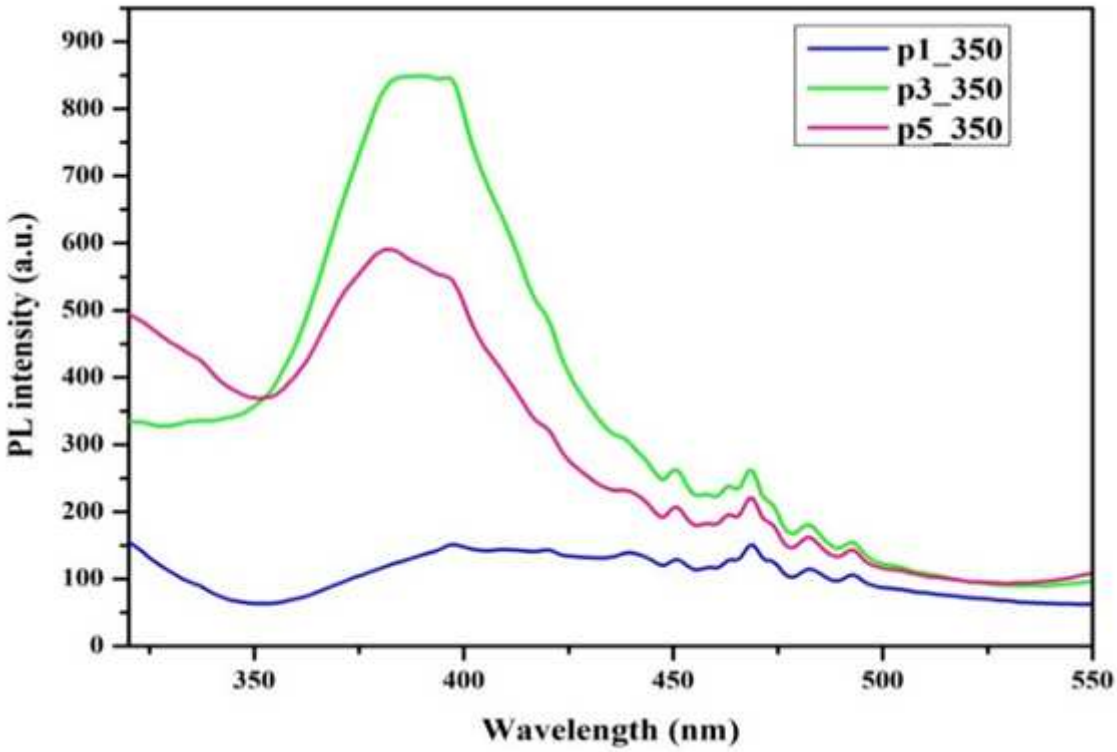

Figure 7

PL Spectra of TiO2

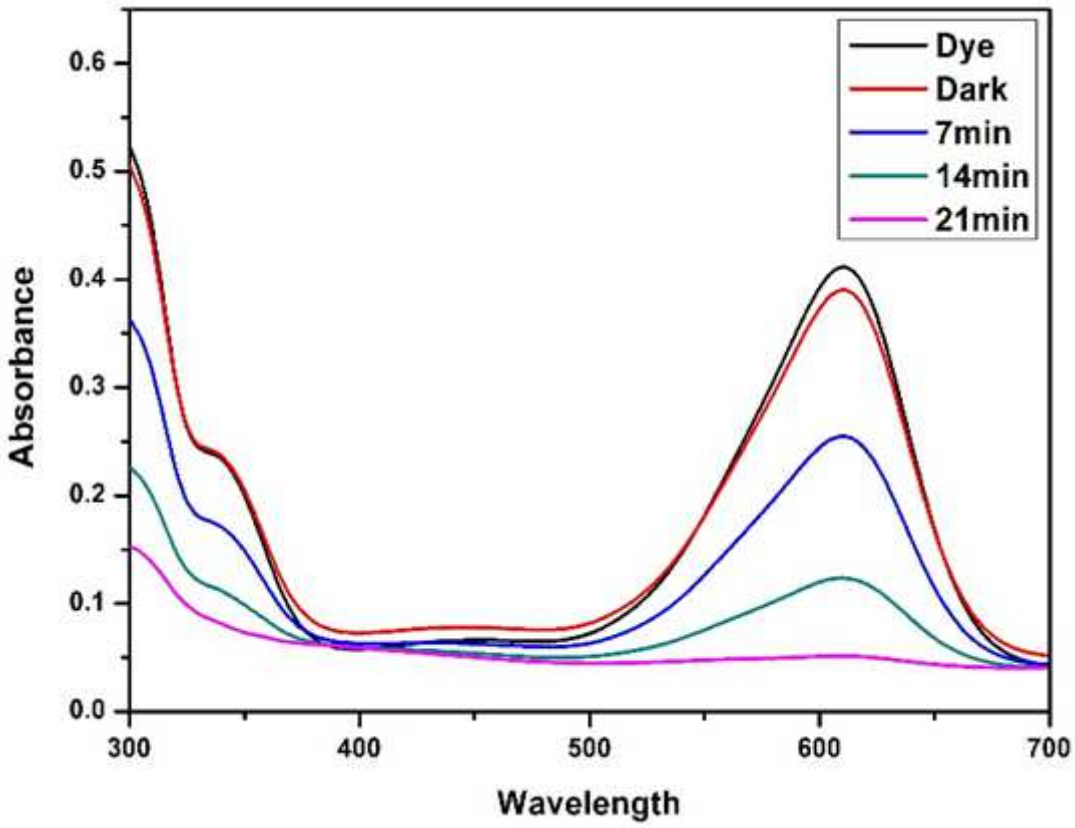

Figure 8

Absorbance spectra of IC dye

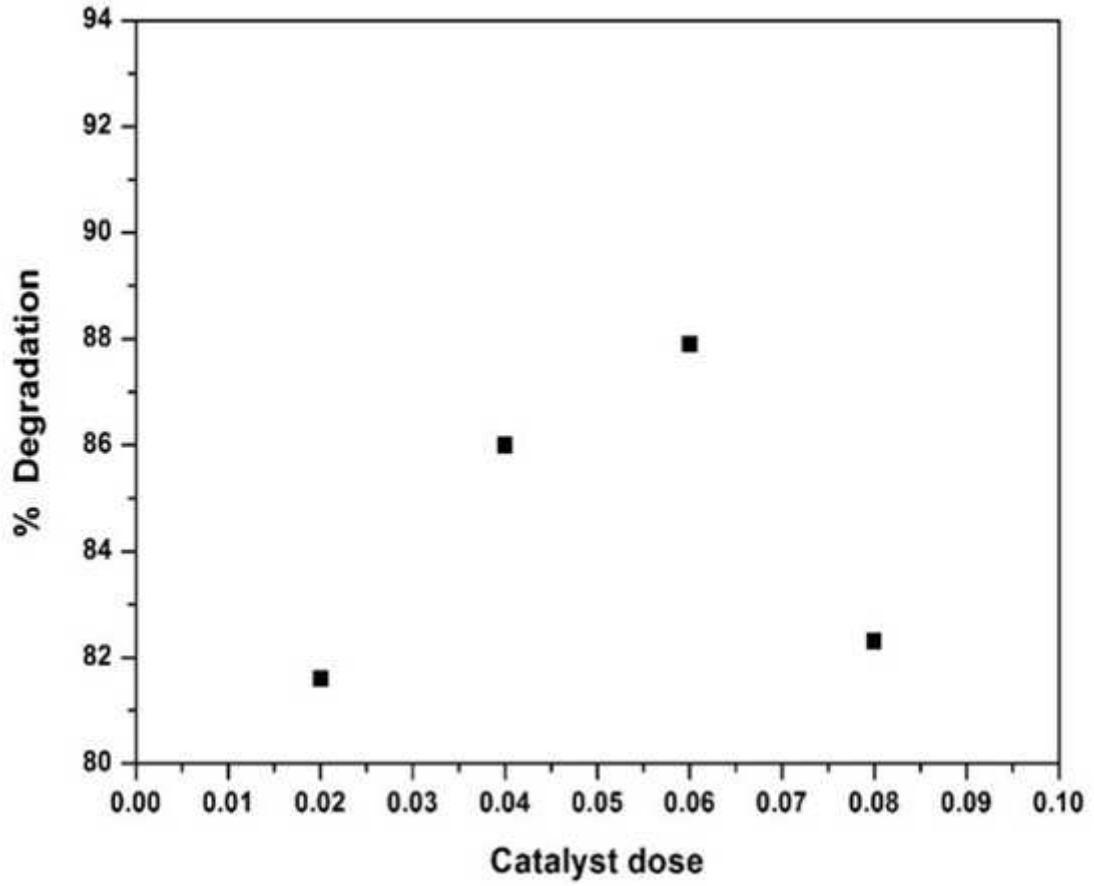

Figure 9

Effect of catalyst dose on degradation efficiency

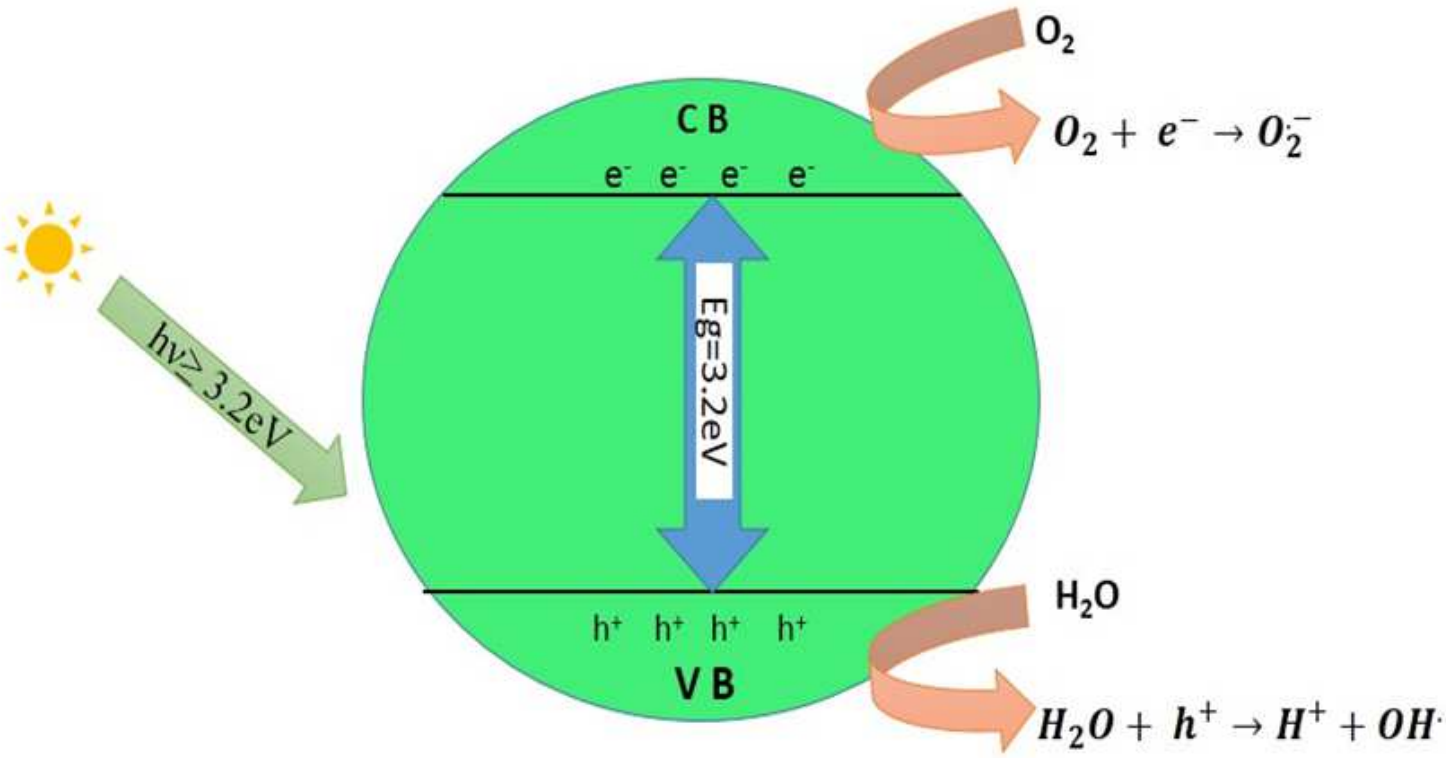

Figure 10

Mechanism of photocatalysis in TiO2